Carbon Nanotube-Graphitic Carbon Nitride Hybrid Films for Flavoenzyme-Catalyzed Photoelectrochemical Cells

Son, Eun Jin; Lee, Sahng Ha; Kuk, Su Keun; Pesic, Milja; Choi, Da Som; Ko, Jong Wan; Kim, Kayoung; Hollmann, Frank; Park, Chan Beum

DOI
10.1002/adfm.201705232

Publication date
2017

Document Version
Accepted author manuscript

Published in
Advanced Functional Materials

ADVANCED FUNCTIONAL MATERIALS

Revised Manuscript

INVITED CONTRIBUTION
DOI: 10.1002/(please add manuscript number)

Carbon Nanotube-Graphitic Carbon Nitride Hybrid Film for Flavoenzyme-Catalyzed Photoelectrochemical Cell

*Eun Jin Son, Sahng Ha Lee, Su Keun Kuk, Milja Pesic, Da Som Choi, Jong Wan Ko, Kayoung Kim, Frank Hollmann, Chan Beum Park**

---

[*] E. J. Son, Dr. S. H. Lee, S. K. Kuk, D. S. Choi, J. W. Ko. K. Kim, Prof. Dr. C. B. Park
Department of Materials Science and Engineering
Korea Advanced Institute of Science and Technology (KAIST)
335 Science Road, Daejeon 305-701, Republic of Korea
E-mail: parkcb@kaist.ac.kr

Dr. M. Pesic, Prof. Dr. F. Hollmann
Department of Biotechnology, Delft University of Technology, Van der Maasweg 9, 2629 HZ Delft, The Netherlands.

[**] This work was supported by the National Research Foundation (NRF) *via* the Creative Research Initiative Center (Grant number: NRF-2015 R1A3A2066191), Republic of Korea, and the Netherlands Organisation for Scientific Research by a VICI grant (Grant number: 724.014.003).

‡ Supporting Information is available on the WWW under http://www.journal.com or from the author.

ABSTRACT

In green plants, solar-powered electrons are transferred through sophistically arranged photosystems and are subsequently channelled into the Calvin cycle to generate chemical energy. Inspired by the natural photosynthetic scheme, we have constructed a photoelectrochemical cell (PEC) configured with protonated graphitic carbon nitride (p-g-C_3N_4) and carbon nanotube hybrid (CNT/p-g-C_3N_4) film cathode and FeOOH-deposited bismuth vanadate (FeOOH/$BiVO_4$) photoanode for the production of industrially useful chiral alkanes using an old yellow enzyme homologue from *Thermus scotoductus* (TsOYE). In the biocatalytic PEC platform, photoexcited electrons provided by the FeOOH/$BiVO_4$ photoanode are transferred to the robust and self-standing CNT/p-g-C_3N_4 hybrid film that electrocatalytically reduces flavin mononucleotide (FMN) mediator. The p-g-C_3N_4 promoted a two-electron reduction of FMN coupled with an accelerated electron transfer by the conductive CNT network. The reduced FMN subsequently delivered the electrons to TsOYE for the highly enantioselective conversion of ketoisophorone to (R)-levodione. Under light illumination (> 420 nm) and external bias, (R)-levodione was synthesized with the enantiomeric excess value of above 83%, not influenced by the scale of applied bias, simultaneously exhibiting stable and high current efficiency. Our results suggest that the biocatalytic PEC made up of economical materials can selectively synthesize high-value organic chemicals using water as an electron donor.

Keywords: graphitic carbon nitride, carbon nanotube, photoelectrochemical cell, artificial photosynthesis, biocatalysis

1. Introduction

Green plants operate elaborate photosystems in a beautiful harmony to convert sunlight into chemical energy through photoinduced electron transfer. During natural photosynthesis, photosystem II (PS II) captures light energy to extract electrons and protons from water oxidation and the photoexcited electrons move to photosystem I (PS I), achieving additional reducing power by a second light absorption. In the PS I, a flavoenzyme called ferredoxin-nicotinamide adenine dinucleotide phosphate ($NADP^+$) reductase catalyzes the reduction of oxidized $NADP^+$, which is subsequently utilized by redox biocatalysts to produce sugars and other organic chemicals in the Calvin cycle (Scheme 1A).[1-3] In the past decades, many researchers have made efforts to construct artificial photosynthetic platforms by simplifying the complex scheme of natural electron transfer.[4-6] For successful implementation of artificial photosynthesis, it is critical to design i) a light-harvesting module, ii) forwarding the electrons with minimal charge recombination, and iii) an efficient catalytic cycle.

For the first two requirements, a photoelectrochemical cell (PEC) configured with photoelectrodes can be a desirable option because it can deliver photoexcited electrons through an external wire to minimize back electron transfer.[7-9] For light-driven electrochemical water oxidation, n-type bismuth vanadate ($BiVO_4$) has been regarded as a top-performer photoanode material among other semiconductors.[10-13] It has adequate light absorption efficiency due to its relatively small band gap (~2.4 eV), and shows superior photochemical stability in aqueous electrolyte. Although $BiVO_4$-based photoanodes have been intensively studied for solar water oxidation, matching them with a counter part for photosynthesis remains a challenging work. In this study, we explore the feasibility of graphitic carbon nitride (g-C_3N_4) and carbon nanotube hybrid (CNT/g-C_3N_4) as an effective cathode material for biocatalytic production of high-value organic chemicals, using electrons

extracted from water oxidation at the $BiVO_4$ photoanode. The g-C_3N_4 holds a great promise as a catalytic material[14, 15] for oxygen reduction/oxidation reactions in fuel cells,[16, 17] solar water splitting,[18-21] and photocatalytic dye degradation[22, 23] due to its appealing electronic structure, high physicochemical stability, and earth abundance.[24] Regarding the implementation of efficient catalytic cycle, redox enzymes provide an opportunity to transform a wide range of substrates to high-value organic chemicals with unparalleled high selectivity under mild conditions.[25] However, biocatalytic photosynthesis today is still in its infancy due to the intricacy in kinetic coupling of biocatalysis with photocatalysis. For example, organic chemicals such as triethanolamine and ethylenediaminetetraacetic acid are used as sacrificial electron donor, but the accumulation of an oxidized donor impedes continuous progress of the catalytic reactions. In this regard, the use of water as an electron donor is highly desirable for sustainable supply of electrons in a similar way to the natural photosynthesis.

Herein, we report a biomimetic PEC that is configured with a $BiVO_4$-based photoanode and a CNT/g-C_3N_4 cathode using a flavin-containing old yellow enzyme homologue from *Thermus scotoductus* (TsOYE) as a model redox enzyme. TsOYE is a powerful enzyme that can catalyze asymmetric reduction of C=C bonds, producing industrially useful chiral alkanes, with the aid of flavin mononucleotide (FMN) as a redox mediator.[26, 27] As depicted in Scheme 1B, the electrons generated by photoelectrochemical water oxidation at the $BiVO_4$-based photoanode, under visible light irradiation (> 420 nm), are transferred to the CNT/g-C_3N_4 cathode that reduces FMN mediator electrocatalytically. Our study demonstrates that g-C_3N_4 can accelerate FMN reduction when coupled with the facilitated electron transfer by the conductive CNT. Finally, the reduced FMN returns to its initial state

after providing two electrons to TsOYE that catalyzes enantioselective conversion of ketoisophorone to (R)-levodione.

2. Results and discussion

To synthesize nanoporous $BiVO_4$, we electrodeposited BiOI on an ITO electrode, then applied dimethyl sulfoxide solution containing vanadyl acetylacetonate to the BiOI layer, followed by heating at 450 °C for 2 h according to the literature.[13] We further deposited FeOOH (as a water oxidation co-catalyst) on the $BiVO_4$ photoanode using a photo-assisted electrochemical deposition method. According to the literature,[28] the FeOOH layer is amorphous with a short-range order of γ-FeOOH phase. The SEM and TEM images in Figures 1A and 1B show a FeOOH layer (of approximately 3 nm thickness) coated onto $BiVO_4$ nanoparticles (Figure S1). To investigate the surface state and the chemical composition, we recorded an X-ray photoelectron spectroscope (XPS) spectrum of $BiVO_4$ and FeOOH/$BiVO_4$. After the surface modification by FeOOH, Fe 2p signal was newly detected as compared to bare $BiVO_4$ (Figure S2), which revealed the oxidation of Fe^{2+} to Fe^{3+} during the photo-assisted electrodeposition process. The O 1s spectrum of FeOOH/$BiVO_4$ indicates that a major portion of hydroxyl group (OH^-, ~530.32 eV) and a minor portion of O^{2-} (~529.08 eV) species coexisted due to the deposited FeOOH (Figure 1C), which is in well agreement with the literatures.[29, 30] Note that the peak associated with H_2O was due to water molecules chemisorbed FeOOH. The two peaks associated with lattice oxygen (Bi-O, ~529.76 eV) and adsorbed oxygen (~531.49 eV) were observed in the O 1s spectrum of $BiVO_4$ (Figure S3).[31, 32] Energy-dispersive X-ray (EDX) elemental mapping of Fe atoms indicated that Fe was coated conformally on the surface of $BiVO_4$ (Figure S4). Fe atoms were detected in the EDX spectrum only after the deposition process (Figure S5), which confirms

the formation of a FeOOH layer. Next, we examined the properties of FeOOH/$BiVO_4$ as a photoanode material to drive water oxidation under Xe lamp irradiation at 450 W with a 420 nm cut-off filter. The linear-sweep voltammogram (Figure 1D) of $BiVO_4$ photoanode under dark and light conditions in a phosphate buffer (pH 7) indicates that visible-light irradiation induced significant cathodic shift (~1.39 V) of the onset potential for water oxidation due to anodic photocurrent generation in $BiVO_4$. Furthermore, FeOOH/$BiVO_4$ showed 5.11 times higher photocurrent density (0.87 mA cm^{-2}) than bare $BiVO_4$ at 0.6 V (vs. Ag/AgCl), as well as cathodically shifted water oxidation onset potential (~210 mV). The accelerated water oxidation is attributed to the capability of FeOOH cocatalyst to capture photogenerated holes from $BiVO_4$, suppressing charge recombination and reducing the kinetic barrier for water oxidation.[28, 33] This should result in the decreased resistance between the electrode interface and the electrolyte, promoting electron transfer and achieving photocurrent increase and the cathodic shift of onset potential.[34, 35]

We synthesized a self-standing g-C_3N_4 and CNT hybrid film as a cathode material for electron transport to redox biocatalytic components. Prior to making the composite film, we treated g-C_3N_4 with a concentrated hydrochloric acid solution to produce protonated g-C_3N_4 (p-g-C_3N_4) for electrostatically driven assembly with multi-wall CNT fibers (Figure S6). According to the literature,[36] proton-functionalization of g-C_3N_4 allows for better dispersion and higher surface area than non-protonated g-C_3N_4. The better dispersibility and higher surface area should make it easier to exfoliate p-g-C_3N_4. The hybridization of CNT with p-g-C_3N_4 through non-covalent interactions (e.g., electrostatic and π–π interaction) can improve surface contact, leading promoted electron transfer. The positively charged p-g-C_3N_4 (zeta potential: +19.1 mV) and the negatively charged CNT (zeta potential: -6.02 mV) were rigorously mixed using a homogenizer for 15 min, followed by sonication for 1 h. Note that

surface groups such as carboxyl and hydroxyl groups in the pristine CNT, which were represented in the XPS spectrum for C 1s region (Figure S8), should be responsible for the negative charge. Subsequently, a self-standing, CNT/p-g-C_3N_4 film was fabricated by vacuum-filtrating the mixture solution through an anodic aluminum oxide (AAO) membrane (Figure 2A). The comparison of full-range survey XPS scans of CNT/p-g-C_3N_4 and pristine CNT showed that the peak corresponding to N atom appeared for the hybrid film (Figure S7); the estimated C/N atomic ratio was 8.17 in CNT/p-g-C_3N_4 film, whereas N atom was not detected in the pristine CNT film. The main peak related to C=N-C bonding in the N 1s spectrum was split into two peaks (i.e., 398.88 and 398.32 eV), which is due to strong interaction of N atom in g-C_3N_4 with CNT (Figure 2B).[16] Due to the inherent chemical structure of g-C_3N_4, the peak at 400.04 eV related to N atoms in $N(-C)_3$ was observed.[37] Note that the minor peak at 405 eV originated from positively charged CN heterocycles and cyano groups in p-g-C_3N_4.[17] In addition, the C 1s spectrum of CNT/p-g-C_3N_4 in Figure S8A shows a peak at 288.87 eV that was resulted from sp^2-bonded C atoms in g-C_3N_4 assembled with CNT,[17] whereas other peaks representing C=C (284.17 eV), C-C (284.84 eV), C-OH (286.05 eV), and O=C-OH (289.48 eV) bonds originated from the CNT (Figure S8B).[38] The coupling between CNT and p-g-C_3N_4 was further confirmed by Raman spectroscopic analysis, a highly reliable tool for the characterization of carbon-based materials. Figure 2C reveals that both D- and G-band of the unmodified CNT (1344 and 1575 cm^{-1}, respectively) were red-shifted after its hybridization with p-g-C_3N_4 (1346 and 1579 cm^{-1}). The apparent band-shift of the Raman band indicates the charge transfer between CNT and p-g-C_3N_4, which can promote electron transfer between the two functional materials.

We examined the coupling effect of p-g-C_3N_4 and CNT on FMN reduction in a three-electrode configuration. As indicated in Scheme 1B, FMN reduction is the first step of

cathodic electron transfer toward enantioselective reduction by TsOYE. Our cyclic voltammetric analysis indicated superior electrocatalytic activity of CNT/p-g-C_3N_4 hybrid film for the reduction of FMN (Figure 3A). We detected a positive shift of approximately 137 mV in the reduction potential of FMN, as well as much higher peak current density at the CNT/p-g-C_3N_4 film than pristine CNT film. To obtain further insights about the kinetics of FMN reduction at the CNT/p-g-C_3N_4 film surface, we carried out the Tafel analysis (Figure 3B). The Tafel slope of the CNT/p-g-C_3N_4, which was derived from the partial current density associated with FMN reduction, was measured to be 190 mV dec^{-1}, whereas the slope of pristine CNT cathode was 246 mV dec^{-1}. The much smaller Tafel slope indicates faster electron transfer kinetic at the CNT/p-g-C_3N_4 surface than pristine CNT electrode. On the other hand, compared to a bare glassy carbon (GC) electrode, p-g-C_3N_4 showed not only higher peak current density, but also positively shifted value of $E_{1/2}$ by approximately 38 mV in FMN reduction (Figure S9A). Pristine CNT on GC did not show any significant change in $E_{1/2}$, but exhibited higher peak current density due to the metallic conductivity of CNT (Figure S9B). The conduction band edge of p-g-C_3N_4 lies at -0.55 V (vs. NHE at pH 7),[39] which is higher than the reduction potential of FMN (-0.243 V vs. NHE at pH 7). Thus, under an applied bias, energized electrons from CNT can be transferred to oxidized FMN via p-g-C_3N_4, which should participate in the two-electron reduction of FMN. Taken together, the results suggest that the accelerated FMN reduction at the CNT/p-g-C_3N_4 hybrid film originated from the electrocatalytic activity of p-g-C_3N_4 with the aid of facile electron transfer by the conductive CNT scaffold.

We further investigated whether the enhanced electron transfer from CNT/p-g-C_3N_4 can facilitate the reduction of FMN. The test was performed in a half-cell configuration (i.e., CNT/p-g-C_3N_4 or pristine CNT film as a working electrode, Ag/AgCl as a reference

electrode, and Pt wire as a counter electrode). Under an applied bias of -0.5 V (vs. Ag/AgCl) at CNT/p-g-C_3N_4 cathode, two FMN absorbance peaks at 445 and 373 nm simultaneously decreased while one isosbestic point at 356 nm was observed, which indicates that FMN was reduced by accepting two electrons from the hybrid film cathode (Figure 4A).[26] In contrast, there was a negligible change in the absorbance of FMN with pristine CNT film, showing that FMN was not reduced at the CNT electrode (Figure 4B). The apparent difference in the capability of FMN reduction between CNT/p-g-C_3N_4 and CNT further confirms the fact that the hybrid film promoted electrocatalytic reduction of FMN that would subsequently mediate the TsOYE catalysis.

To explore the capability of CNT/p-g-C_3N_4 film cathode to deliver photoexcited electrons to TsOYE via the FMN mediator, we carried out linear-sweep voltammetric analysis. As shown in Figure 4C, cathodic current increased by the sequential addition of FMN and TsOYE, which indicates that electrons were efficiently transferred from CNT/p-g-C_3N_4 to TsOYE via FMN. We further confirmed highly stereoselective, TsOYE-catalyzed reduction of ketoisophorone by the CNT/p-g-C_3N_4 cathode in the half-cell configuration (Figure 4D). Under an applied bias of -0.5 V (vs. Ag/AgCl) at 50 $^{\circ}$C for 2 h, 2.33 mM of (R)-levodione was synthesized from ketoisophorone with an enantiomeric excess (ee) of 84.21%. Note that no product was detected by the pristine CNT cathode under the same experimental condition due to the lack of reducing power of the CNT film toward FMN reduction. The significantly higher current flow from CNT/p-g-C_3N_4 than pristine CNT during the biocatalytic reaction (Figure S10) further supported the fact that the hybrid film facilitated selective electron transport to FMN.

We assembled a full PEC by wiring FeOOH/$BiVO_4$ photoanode to CNT/p-g-C_3N_4 film cathode in a two-electrode configuration, so as to employ water as an electron donor for flavoenzyme-catalyzed photosynthesis. Light-driven electrochemical water oxidation at the FeOOH/$BiVO_4$ photoanode provided photoexcited electrons that were consumed in the cathodic reaction. As shown in Figure 5A, no current flowed through the PEC under dark conditions, whereas light irradiation (> 420 nm) to the FeOOH/$BiVO_4$ photoanode generated significantly increased photocurrent. To analyze the degree of external energy input to the PEC system, we estimated the solar-to-FMN reduction efficiency according to external applied bias photon-to-current efficiency (EABPE). In the FMN reduction system, EABPE was calculated using the following equation: EABPE = [$|j|$ (mA cm^{-2}) × (V_{th}-V_{bias}) (V) × P_{total}^{-1} (mW cm^{-2})$^{-1}$] x 100, where V_{th} (1.04 V) is a theoretical voltage difference between water oxidation and FMN reduction potential at neutral pH, P_{total} (70 mW cm^{-2}) is total incident light intensity, and j is photocurrent density under the external bias of V_{bias}. The highest EABPE of 0.051% was achieved at an external bias of 0.46 V (Figure S11). Subsequently, the FMN-reducing PEC was coupled with TsOYE for asymmetric reduction of C=C bonds of ketoisophorone. We observed that ketoisophorone (10 mM) was converted to (R)-levodione (2.13 mM after 2 h reaction) at the production rate of 1.06 mM h^{-1} (ee: 87.59%) under the applied bias of 0.5 V (Figure 5B), which rate is more than three-fold higher than the previously reported value using an electrochemical system.[40] Furthermore, the high enantioselectivity indicates that most electrons transferred from CNT/p-g-C_3N_4 film cathode to FMN participated in the catalytic reduction of ketoisophorone by TsOYE. Note that, without TsOYE, racemic product was formed with 0% ee, whereas the enantioselectivity for the synthesis of (R)-levodione remained at above 74% ee in the presence of TsOYE (Figure 5C). The Faradaic efficiency was estimated to be 81.13% under 0.5 V applied voltage and the

current flow during the reaction was maintained at approximately 89.87% of the initial value on average (Figure S12). The Faradaic efficiency was calculated according to the following equation: Faradaic efficiency (%) = αnF/Q x 100, where α (mol) is the amount of produced (R)-levodione, n is the number of electrons needed for the synthesis of (R)-levodione (n = 2), F is the Faraday constant (F = 96,485 C mol^{-1}), and Q (C) is the total charge passed during the reaction. We attribute the stable and high current efficiency to the absence of O_2 in the electrolysis reaction. Low current efficiency has been a critical issue in electroenzymatic synthesis using O_2-dependant biocatalysts because of the difficulties in coupling cathodic reduction of mediators to the enzymatic oxidation reaction. Particularly, direct cathodic reduction of O_2 and O_2-related reoxidation of the mediators impair the efficient usage of reducing equivalents provided by the cathode.[41] The conversion efficiency for 2 h in terms of external bias showed a similar tendency with the estimated EABPE (Figure 5D); the conversion yield increased with the increasing bias up to 0.8 V achieving the highest conversion rate of 1.28 mM h^{-1} on average. The enantioselectivity was not affected by the scale of the external bias, which remained at above 83%. Taken together, the results show that the photoinduced electrons generated from FeOOH/$BiVO_4$ were effectively transferred to CNT/p-g-C_3N_4 with an aid of external bias, where most of the electrons were used for FMN-mediated, TsOYE catalysis to produce (R)-levodione with a remarkable enantioselectivity.

3. Conclusion

We have synthesized a robust p-g-C_3N_4 and CNT hybrid film as a self-standing cathode material for selective transport of photoexcited electrons to flavin-mediated biocatalytic components. Inspired by the scheme of natural photosynthesis, a biomimetic PEC composed of CNT/p-g-C_3N_4 film cathode and FeOOH/$BiVO_4$ photoanode has been developed by

employing TsOYE as an enantioselective redox catalyst and using water as an electron donor. The CNT/p-g-C_3N_4 film cathode consumed electrons supplied by the photoanode for highly selective, TsOYE-catalyzed reduction of ketoisophorone to (R)-levodione. Under light illumination (> 420 nm) and an applied bias of 0.5 V, (R)-levodione was synthesized at the production rate of 1.06 mM h^{-1} and an ee of 87.59%. The high enantioselectivity indicates that photoexcited electrons were effectively transferred from CNT/p-g-C_3N_4 to FMN and then to TsOYE. Furthermore, high current efficiency was achieved with a Faradaic efficiency of 81.13% on average at 0.5 V, which is attributed to O_2-independent TsOYE, avoiding the oxygen dilemma issue in conventional electroenzymatic synthesis. Our results suggest that the deliberate integration of CNT/p-g-C_3N_4 hybrid film-based PEC with flavin-mediated redox enzymes can produce industrially valuable chiral alkane using solar-powered electrons that are sustainably supplied from inexpensive materials.

4. Experimental section

Chemicals

All chemicals, including bismuth(III) nitrate pentahydrate [$Bi(NO_3)_3 \cdot 5H_2O$], potassium iodide (KI), absolute ethanol, *p*-bezoquinone, nitric acid [HNO_3], dimethyl sulfoxide solution (DMSO), vanadyl acetylacetonate [$VO(acac)_2$], iron(II) sulfate heptahydrate ($FeSO_4$), urea, hydrochloric acid (HCl), multi-wall CNT, riboflavin 5'-monophoaphate sodium salt hydrate (FMN), ketoisophorone, and MOPS were purchased from Sigma-Aldrich (St. Louis, MO, USA).

Synthesis of FeOOH/ $BiVO_4$ photoanode

The FeOOH-deposited $BiVO_4$ (FeOOH/$BiVO_4$) electrode was fabricated according to the literature.[13] Firstly, we adjusted the pH of a 0.04 M of $Bi(NO_3)_3$ $5H_2O$ in a 0.4 M KI solution (50 ml) to 1.7 using HNO_3 and then added absolute ethanol (20 ml) containing 0.23 M *p*-benzoquinone to the solution, followed by vigorous stirring for few minutes. Afterwards, BiOI was electrodeposited on ITO substrate in a 3-electrode configuration using ITO as a working electrode, Ag/AgCl as a reference electrode, and Pt wire as a counter electrode; an ITO (1 x 4 cm^2) substrate was immersed in the as-prepared reaction mixture under the applied bias of -0.1 V (vs. Ag/AgCl) for 4 min at room temperature, followed by washing several times with deionized (DI) water. To make $BiVO_4$ from the BiOI, a 0.2 ml DMSO solution containing 0.2 M of $VO(acac)_2$ was dropped onto the BiOI electrode (1 x 4 cm^2) and the sample was heated at 450 °C with the heating rate of 2 °C min^{-1} for 2 h under air. Subsequently, the sample was immersed in a 1 M NaOH solution for 30 min with gentle stirring to remove excess V_2O_5, followed by rinsing with DI water and drying at room temperature. For the deposition of FeOOH onto the $BiVO_4$ electrode, photo-assisted electrochemical deposition method was applied. The $BiVO_4$ electrode as a working electrode in the 3-electrode configuration (with Ag/AgCl as a reference and Pt wire as a counter electrode) was immersed in a 0.1 M $FeSO_4$ solution with gentle stirring. Prior to the deposition, the solution was purged with N_2 gas for 1 h. Under light illumination to the back-side of the $BiVO_4$ electrode, the bias of 0.25 V (vs. Ag/AgCl) was applied for 20 min. Afterwards, electrochemical deposition of FeOOH was performed by applying the bias of 1.2 V (vs. Ag/AgCl) for 1 min.

Synthesis of CNT/p-g-C_3N_4 film cathode

To synthesize g-C_3N_4 powder, urea (10 g) was dissolved in ultrapure water (5 ml). Subsequently, the solution was placed in an alumina crucible and heated to 550 °C for 3 h at the rate of 0.5 °C min^{-1}. Afterwards, the product was washed with DI water several times and collected to make g-C_3N_4 powder. The CNT/g-C_3N_4 film was fabricated through vacuum filtration of multi-wall CNT and g-C_3N_4 mixture. Prior to make the film, g-C_3N_4 was protonated using 12 M HCl solution to obtain positive-charged powder; 200 mg of g-C_3N_4 in 5 ml HCl was vigorously stirred for 1 h, followed by washing with DI water and ethanol. The protonated g-C_3N_4 (20 mg) in 15 ml ethanol was homogenized for 5 min and multi-wall CNT (10 mg) in 15 ml ethanol was also homogenized for 5 min. Then, the protonated g-C_3N_4 dispersion was mixed with the multi-wall CNT solution, and the mixture was further homogenized for another 15 min and sonicated for additional 1 h. The mixture was vacuum-filtrated on an AAO membrane, followed by vacuum drying to fabricate CNT/g-C_3N_4 film. To make CNT/g-C_3N_4 electrode, the film was cut into 1 x 1 cm^2 pieces and was connected by copper wire using silver paste covered by insulating epoxy resin.

TsOYE preparation

Escherichia coli BL21 (DE3) harboring a pET22b(+) plasmid containing the gene encoding for *Ts*OYE was used for the expression of *Ts*OYE. 1 L of autoinduction ZYM-5052 media supplied with 100 µg/mL ampicillin was inoculated with 10 mL of overnight culture and incubated overnight at 37 °C in baffled shake flasks.[42] For the purification of *Ts*OYE, the cell pellet (resulting from centrifugation and washing with 20 mM MOPS buffer pH 7.5 containing 5 mM $CaCl_2$) was suspended in the same buffer. Mechanical cell disruption was effected by using Multi Shot Cell Disruption System (Constant Systems Ltd, Daventry, UK). Cell debris was separated from the crude extract by centrifugation at 10000 x g for 30 min at

4 ˚C. The supernatant was incubated at 70 °C for 1.5 h. Precipitated proteins were separated by centrifugation for 30 min, at 4 ˚C and 8000 x g. Fractions containing *Ts*OYE were collected and incubated with 5 mM FMN. After 30 min of incubation on ice, enzyme suspension was desalted twice using PD-10 Desalting Columns (GE Healthcare) in order to remove the excess of FMN, and concentrated using Amicon® Ultra-15 Centrifugal Filter Device (cutoff 30K). A bright yellow solution of *Ts*OYE (more than 95% pure as estimated by SDS-page analysis) was obtained.

Photoelectroenzymatic reactions and analysis

Photoelectroenzymatic synthesis using water as an electron donor was performed in a two-electrode configuration. The FeOOH/$BiVO_4$ photoanode and CNT/p-g-C_3N_4 cathode were placed in separated compartments that were connected by salt bridge. For water oxidation, the photoanode was immersed in a 10 mM phosphate buffer (pH 7) solution under Xe lamp (Newport Co., USA) irradiation at 450 W with a 420 nm cut-off filter. The total incident light intensity at the reaction vessel was 70 mW cm^{-2}. For electroenzymatic synthesis, the reaction mixture was prepared as following; 0.85 mM FMN, 10 uM TsOYE, and 10 mM ketoisophorone in a 50 mM MOPS buffer solution (pH 7) containing 10 mM $CaCl_2$. The MOPS buffer was continuously purged with N_2 gas (purity of 99.999%) before and during the reaction. The temperature was maintained at 50 °C. Electroenzymatic reaction by a half-cell was performed in the same, TsOYE-containing reaction mixture in a three-electrode configuration using CNT/p-g-C_3N_4 or CNT cathode as a working electrode, Ag/AgCl as a reference electrode, and Pt wire as a counter electrode. At regular intervals, reaction samples (50 μl) were extracted by 200 μl of ethyl acetate containing 5 mM 1-octanol as and internal

standard. After centrifuging for 1 min at 10,000 rpm, the organic phase was dried with magnesium sulfate, followed by repeating the same centrifugation process. The concentration of (R)-levodione in the supernatant was analyzed by a gas chromatography (Agilent Technologies Inc., USA) using a CP-Chirasil-Dex CB column (25 m, 0.32 mm, 0.25 μl).

Spectroscopic analysis of FMN reduction

We compared the capability of FMN reduction at the CNT/p-g-C_3N_4 hybrid film and the pristine CNT film in a half cell configuration (i.e., each film as a working electrode, Ag/AgCl as a reference electrode, and Pt wire as a counter electrode). Each film cathode was immersed in a 50 mM MOPS buffer (pH 7) containing 50 μM of FMN and the external bias of -0.5 V (vs. Ag/AgCl) was applied. Using a spectrophotometer (model V-650, JASCO Inc., Japan), we monitored the degree of FMN reduction by observing the change of FMN absorbance spectra at 445 and 373 nm.

Electrochemical characterization

The voltammetric analyses of each electrode were carried out with a single cell compartment in a three-electrode configuration connected to a potentiostat/galvanostat (WMPG 1000, Wonatech Co., Korea). In all measurements, Ag/AgCl (3 M NaCl) and Pt wire were used as a reference electrode and a counter electrode, respectively. The characterization of FeOOH/$BiVO_4$ photoanode (a working electrode) was performed in a 10 mM phosphate buffer (pH 7) with a scan rate of 20 mV s^{-1}. For the characterization of cathodes, film electrodes or glassy carbon electrodes (diameter of 3 mm) on which 5 μl of solution (e.g., CNT/p-g-C_3N_4, p-g-C_3N_4, or CNT in absolute ethanol) were dropped were analyzed as working electrodes. To obtain linear-sweep voltammetric spectrum of the full-cell, the

$FeOOH/BiVO_4$ (in 10 mM, pH 7 phosphate buffer) and CNT/p-g-C_3N_4 film (in 100 mM, pH 7 phosphate buffer) electrodes were placed in separated compartment cells connected by salt bridge, with or without light illumination to the anodic side. The scan rate was 20 mV s^{-1}. To analyze Tafel plot of CNT/p-g-C_3N_4 and CNT films, linear-sweep voltammetric spectra was obtained at the scan rate of 5 mV s^{-1} in a 100 mM phosphate buffer containing 1 mM FMN.

Materials characterization

The morphology of electrodes were observed using an S-4800 field scanning emission microscope (SEM; Hitachi Co., Japan) and a JEM-3010 transmission electron microscopy (TEM; Jeol Ltd., Japan). Energy dispersive X-ray spectroscopy analysis was performed using the same S-400 field SEM. The chemical composition of the electrodes' surface was analyzed by X-ray photoelectron spectroscopy (XPS; Thermo VG Scientific UK). Raman spectra were collected using a LabRAM HR (Horiba Jobin Yiyon Inc., France) with a resolution of less than 0.7 cm^{-1} with 2400 gr mm^{-1}, using 514 nm laser as light source. Zeta potentials of p-g-C_3N_4 and CNT dispersed in ethanol were measured using Zetasizer Nano ZS (Malvern Ltd., UK).

References

[1] J. Barber, *Chem. Soc. Rev.* **2009**, *38*, 185.

[2] S. H. Lee, J. H. Kim, C. B. Park, *Chem. Eur. J.* **2013**, *19*, 4392.

[3] J. H. Kim, D. H. Nam, C. B. Park, *Curr. Opin. Biotechnol.* **2014**, *28*, 1.

[4] C. Liu, J. J. Gallagher, K. K. Sakimoto, E. M. Nichols, C. J. Chang, M. C. Y. Chang, P. Yang, *Nano Lett.* **2015**, *15*, 3634.

[5] H. Tada, T. Mitsui, T. Kiyonaga, T. Akita, K. Tanaka, *Nat. Mater.* **2006**, *5*, 782.

[6] Y. Tachibana, L. Vayssieres, J. R. Durrant, *Nat. Photon.* **2012**, *6*, 511.

[7] M. G. Walter, E. L. Warren, J. R. McKone, S. W. Boettcher, Q. Mi, E. A. Santori, N. S. Lewis, *Chem. Rev.* **2010**, *110*, 6446.

[8] S. K. Kuk, R. K. Singh, D. H. Nam, R. Singh, J. K. Lee, C. B. Park, *Angew. Chem. Int. Ed.* **2017**, *56*, 3827.

[9] E. J. Son, J. W. Ko, S. K. Kuk, H. Choe, S. Lee, J. H. Kim, D. H. Nam, G. M. Ryu, Y. H. Kim, C. B. Park, *Chem. Commun.* **2016**, *52*, 9723.

[10] Y. Ma, A. Kafizas, S. R. Pendlebury, F. L. Formal, J. R. Durrant, *Adv. Funct. Mater.* **2016**, *26*, 4951.

[11] D. Kang, T. W. Kim, S. R. Kubota, A. C. Cardiel, H. G. Cha, K.-S. Choi, *Chem. Rev.* **2015**, *115*, 12839.

[12] R. Li, H. Han, F. Zhang, D. Wang, C. Li, *Energy. Environ. Sci.* **2014**, *7*, 1369.

[13] T. W. Kim, K.-S. Choi, *Science* **2014**, *343*, 990.

[14] S. Ye, R. Wang, M.-Z. Wu, Y.-P. Yuan, *Appl. Surf. Sci.* **2015**, *358*, 15.

[15] W.-J. Ong, L.-L. Tan, Y. H. Ng, S.-T. Yong, S.-P. Chai, *Chem. Rev.* **2016**, *116*, 7159.

[16] Q. Liu, J. Zhang, *Langmuir* **2013**, *29*, 3821.

[17] T. Y. Ma, S. Dai, M. Jaroniec, S. Z. Qiao, *Angew. Chem. Int. Ed.* **2014**, *53*, 7281.

[18] G. Zhang, Z.-A. Lan, L. Lin, S. Lin, X. Wang, *Chem. Sci.* **2016**, *7*, 3062.

[19] Z. Li, C. Kong, G. Lu, *J. Phys. Chem. C* **2016**, *120*, 56.

[20] D. J. Martin, P. J. T. Reardon, S. J. A. Moniz, J. Tang, *J. Am. Chem. Soc.* **2014**, *136*, 12568.

[21] J. Liu, Y. Liu, N. Liu, Y. Han, X. Zhang, H. Huang, Y. Lifshitz, S.-T. Lee, J. Zhong, Z. Kang, *Science* **2015**, *347*, 970.

[22] C. Li, S. Wang, T. Wang, Y. Wei, P. Zhang, J. Gong, *Small* **2014**, *10*, 2783.

[23] J. Sun, B. V. K. J. Schmidt, X. Wang, M. Shalom, *ACS Appl. Mater. Interfaces* **2017**, *9*, 2029.

[24] B. Kumru, M. Antonietti, B. V. K. J. Schmidt, *Langmuir* **2017**, *33*, 9897.

[25] D. H. Nam, S. K. Kuk, H. Choe, S. Lee, J. W. Ko, E. J. Son, E.-G. Choi, Y. H. Kim, C. B. Park, *Green Chem.* **2016**, *18*, 5989.

[26] S. H. Lee, D. S. Choi, M. Pesic, Y. W. Lee, C. E. Paul, F. Hollmann, C. B. Park, *Angew. Chem. Int. Ed.* **2017**, *56*, 8681.

[27] M. Mifsud, S. Gargiulo, S. Iborra, I. W. C. E. Arends, F. Hollmann, A. Corma, *Nat. Commun.* **2014**, *5*, 3145.

[28] J. A. Seabold, K.-S. Choi, *J. Am. Chem. Soc.* **2012**, *134*, 2186.

[29] J. Liu, M. Zheng, X. Shi, H. Zeng, H. Xia, *Adv. Funct. Mater.* **2016**, *26*, 919.

[30] D. H. Nam, G. M. Ryu, S. K. Kuk, D. S. Choi, E. J. Son, C. B. Park, *Appl. Catal. B* **2016**, *198*, 311.

[31] J. Zhang, Y. Lu, L. Ge, C. Han, Y. Li, Y. Gao, S. Li, H. Xu, *Appl. Catal. B* **2017**, *204*, 385.

[32] J. Gan, X. Lu, B. B. Rajeeva, R. Menz, Y. Tong, Y. Zheng, *ChemElectroChem* **2015**, *2*, 1385.

[33] K. J. McDonald, K.-S. Choi, *Energy. Environ. Sci.* **2012**, *5*, 8553.

[34] Q. Yu, X. Meng, T. Wang, P. Li, J. Ye, *Adv. Funct. Mater.* **2015**, *25*, 2686.

[35] J. Aihua, K. Miao, J. Jinping, Z. Yixin, *J, Semicond.* **2017**, *38*, 053004.

[36] Y. Zhang, A. Thomas, M. Antonietti, X. Wang, *J. Am. Chem. Soc.* **2009**, *131*, 50.

[37] D. Foy, G. Demazeau, P. Florian, D. Massiot, C. Labrugère, G. Goglio, *J. Solid State Chem.* **2009**, *182*, 165.

[38] K. Yu, G. Lu, Z. Bo, S. Mao, J. Chen, *J. Phys. Chem. Lett.* **2011**, *2*, 1556.

[39] C. Ye, J.-X. Li, Z.-J. Li, X.-B. Li, X.-B. Fan, L.-P. Zhang, B. Chen, C.-H. Tung, L.-Z. Wu, *ACS Catal.* **2015**, *5*, 6973.

[40] K. Fisher, S. Mohr, D. Mansell, N. J. Goddard, P. R. Fielden, N. S. Scrutton, *Catal. Sci. Tech.* **2013**, *3*, 1505.

[41] A. Tosstorff, A. Dennig, A. J. Ruff, U. Schwaneberg, V. Sieber, K.-M. Mangold, J. Schrader, D. Holtmann, *J. Mol. Catal. B: Enzym.* **2014**, *108*, 51.

[42] F. W. Studier, *Protein Expr. Purif.* **2005**, *41*, 207.

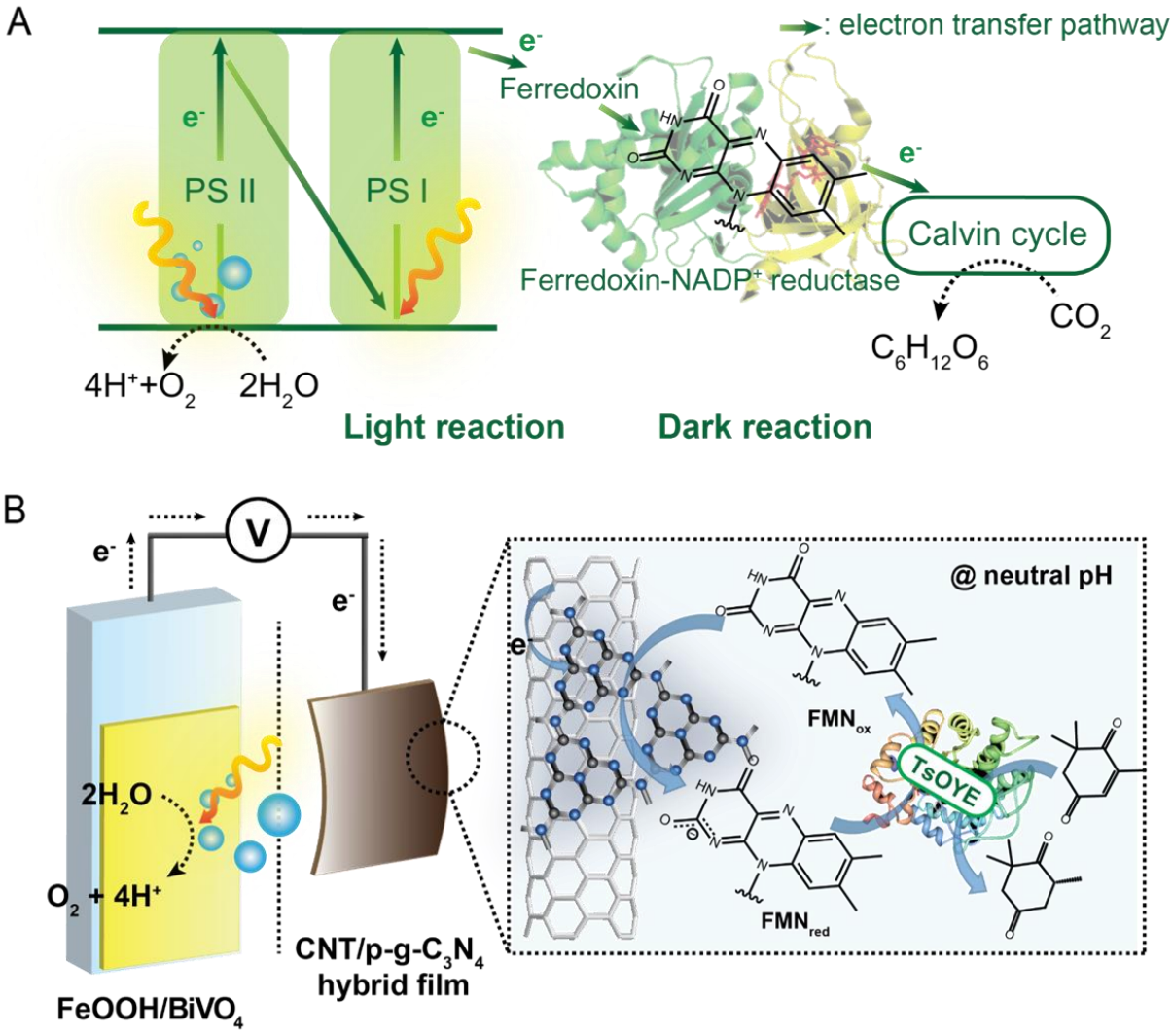

Scheme 1. (A) Electron transfer cascade in natural photosynthesis. The PS II absorbs sunlight and generates electrons and protons through water oxidation and the electrons are transferred to the PS I, followed by capturing second light. In the PS I, a flavoenzyme called ferredoxin-nicotinamide adenine dinucleotide phosphate ($NADP^+$) reductases catalyzes the reduction of oxidized $NADP^+$, which is subsequently used to produce high energy chemicals (e.g., sugars). (B) Under visible light irradiation (> 420 nm), electrons generated by photochemical water oxidation at $FeOOH/BiVO_4$ photoanode are delivered to CNT/p-g-C_3N_4 hybrid film cathode with an aid of external bias. Subsequently, the electrons from the CNT/p-g-C_3N_4 film are used to reduce oxidized FMN, which returns to its initial state after providing two electrons to the flavoenzyme (i.e., TsOYE) that catalyzes enantioselective conversion of ketoisophorone to (R)-levodione.

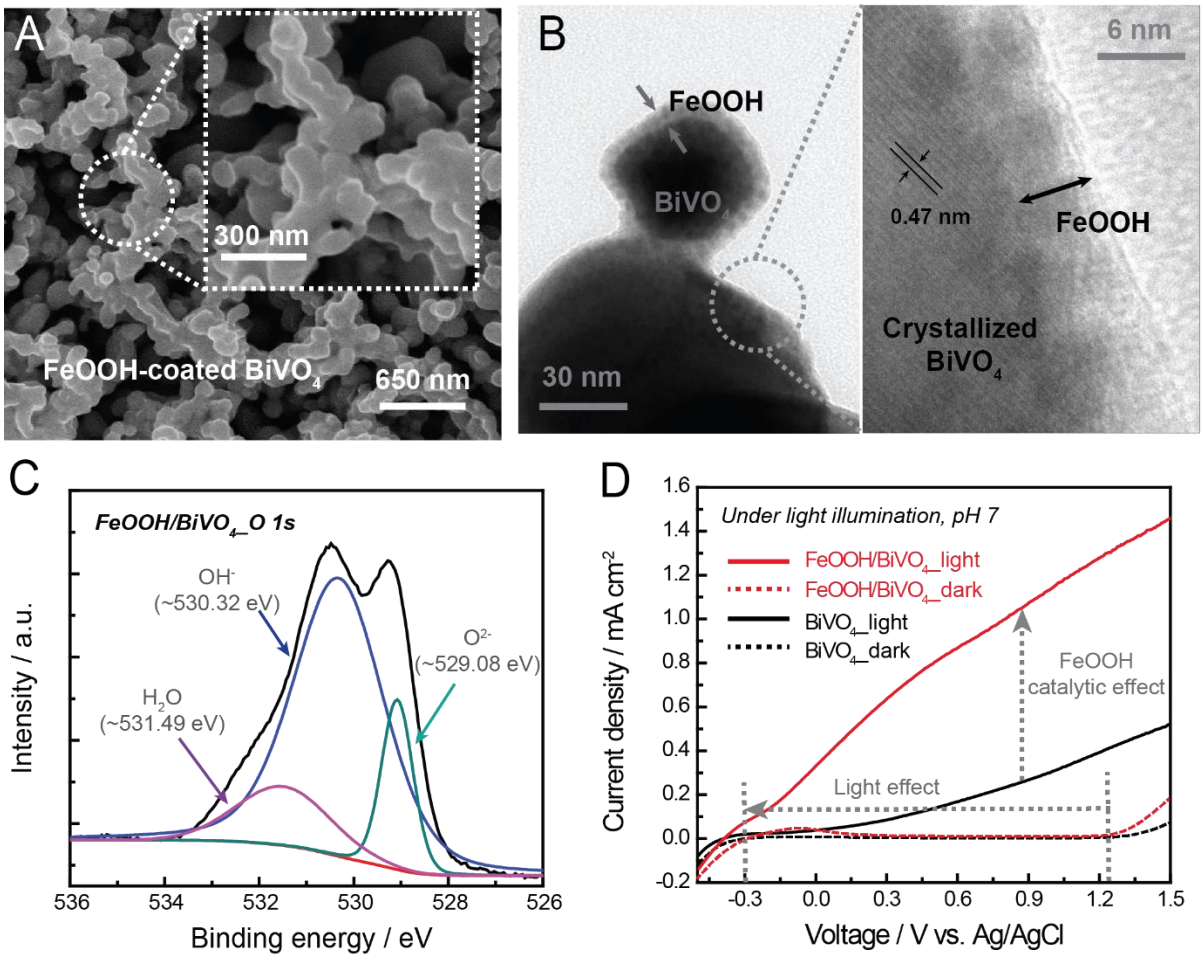

Figure 1. Characterization of $FeOOH/BiVO_4$ photoanode. (A) SEM and (B) TEM images of $FeOOH/BiVO_4$. (C) O1s XPS spectrum of FeOOH that is coated onto $BiVO_4$. (D) Linear-sweep voltammetric spectra of $BiVO_4$ and $FeOOH/BiVO_4$ under dark and light conditions. Throughout the experiments, the light source was Xe lamp at 450 W with a 420 nm cut-off filter. The photoelectrochemical analysis was carried out in a 10 mM phosphate buffer (pH 7) at the scan rate of 20 mV s^{-1}.

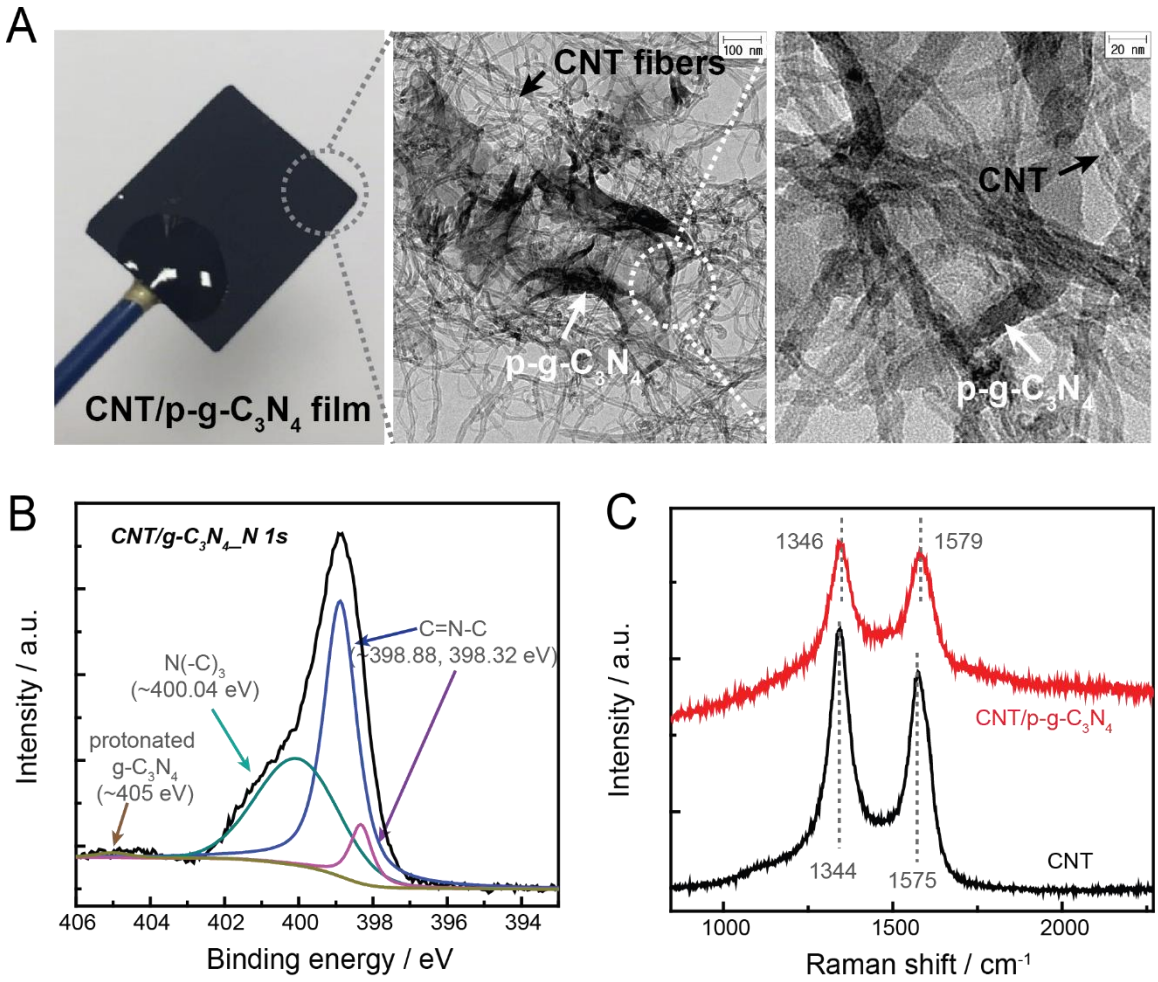

Figure 2. Characterization of CNT/p-g-C_3N_4 hybrid film cathode. (A) Digital camera and TEM images of a CNT/p-g-C_3N_4 film. (B) XPS spectra for N 1s region of the CNT/p-g-C_3N_4 film. (C) Comparison of Raman spectra of CNT/p-g-C_3N_4 and pristine CNT films.

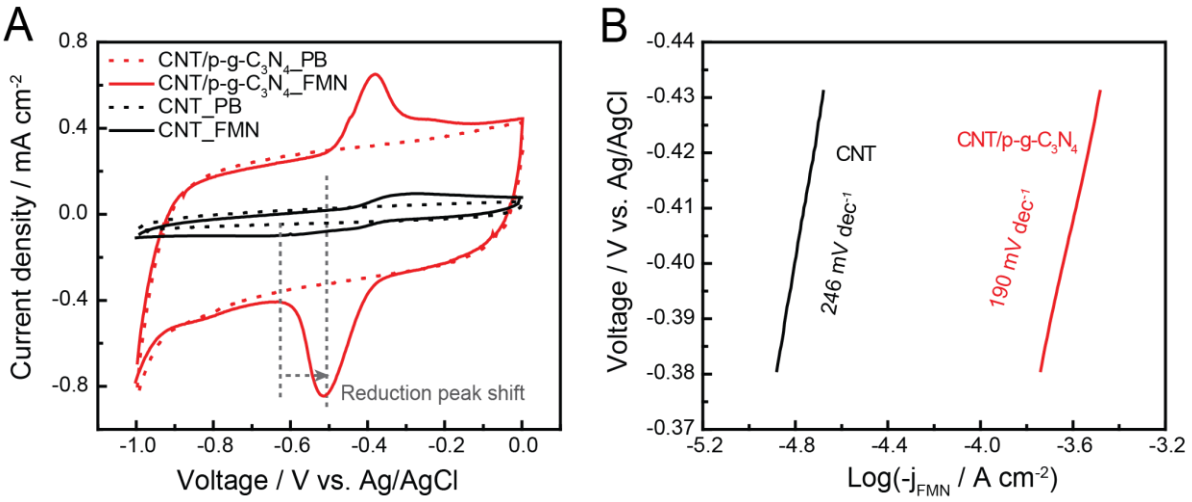

Figure 3. Comparison of electrochemical properties of CNT/p-g-C_3N_4 hybrid film and pristine CNT film on FMN reduction. (A) Cyclic voltammetric spectra of the film electrodes of CNT/p-g-C_3N_4 and CNT in the presence of 1 mM FMN mediator in a 100 mM phosphate buffer solution (pH 7, solid line). Dashed lines indicate the spectra without FMN. Note that the amount of CNT in the CNT/p-g-C_3N_4 and the CNT films was the same. The scan rate was 50 mV s^{-1}. (B) Tafel plots of CNT/p-g-C_3N_4 and CNT film cathode. The scan rate was 5 mV s^{-1}.

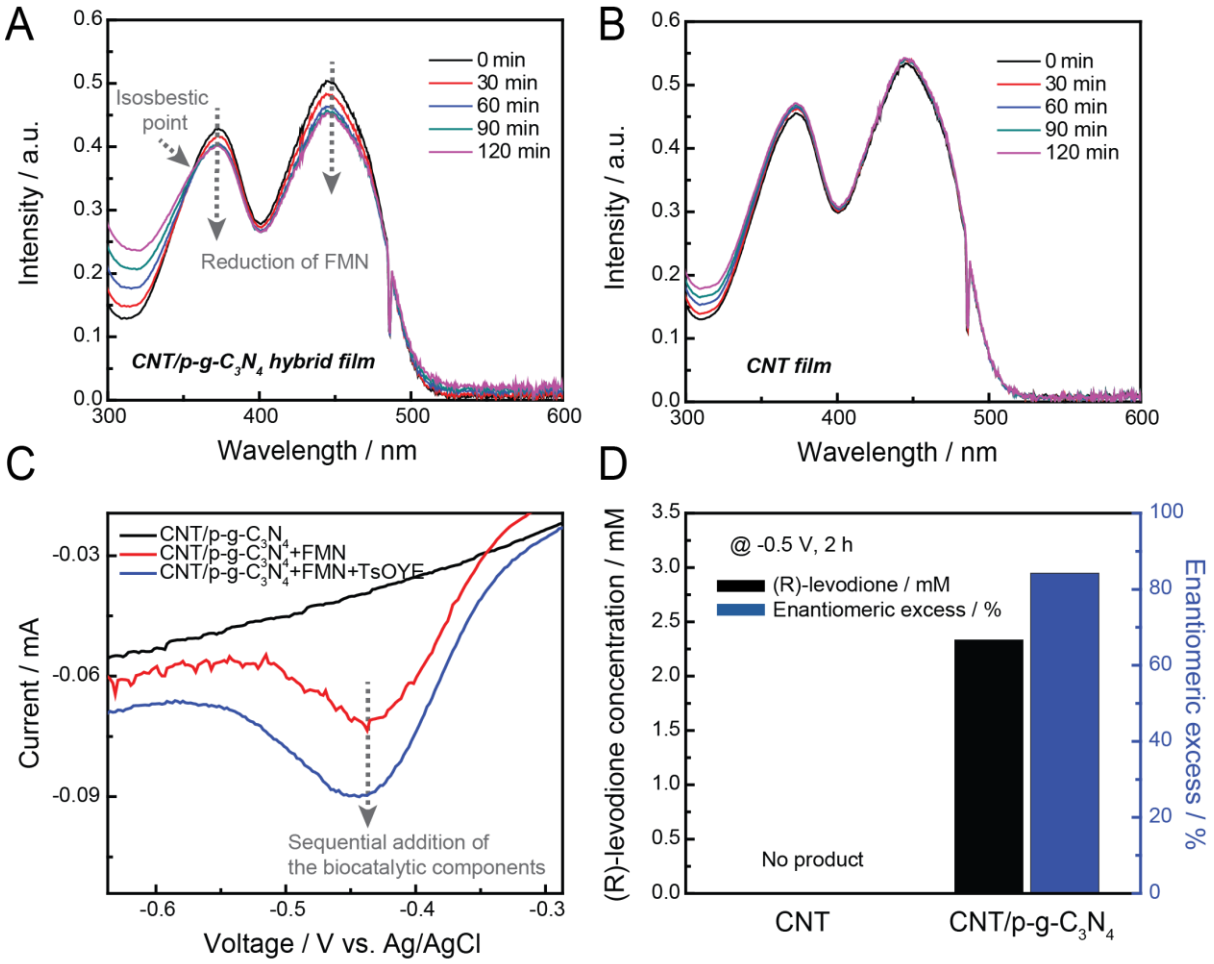

Figure 4. Change of UV-Vis absorbance spectra of FMN at 445 and 373 nm by (A) CNT/p-g-C_3N_4 hybrid film and (B) CNT film. (C) Linear-sweep voltammogram change of CNT/p-g-C_3N_4 with sequential addition of the biocatalytic components (e.g., FMN and TsOYE). The scan rate was 20 mV s^{-1}. (D) TsOYE-catalyzed conversion of ketoisophorone to (R)-levodione by CNT/p-g-C_3N_4 film cathode in comparison to that by pristine CNT film. The experiment was performed in a three-electrode configuration with each cathode as a working electrode, Ag/AgCl as a reference electrode, and Pt wire as a counter electrode.

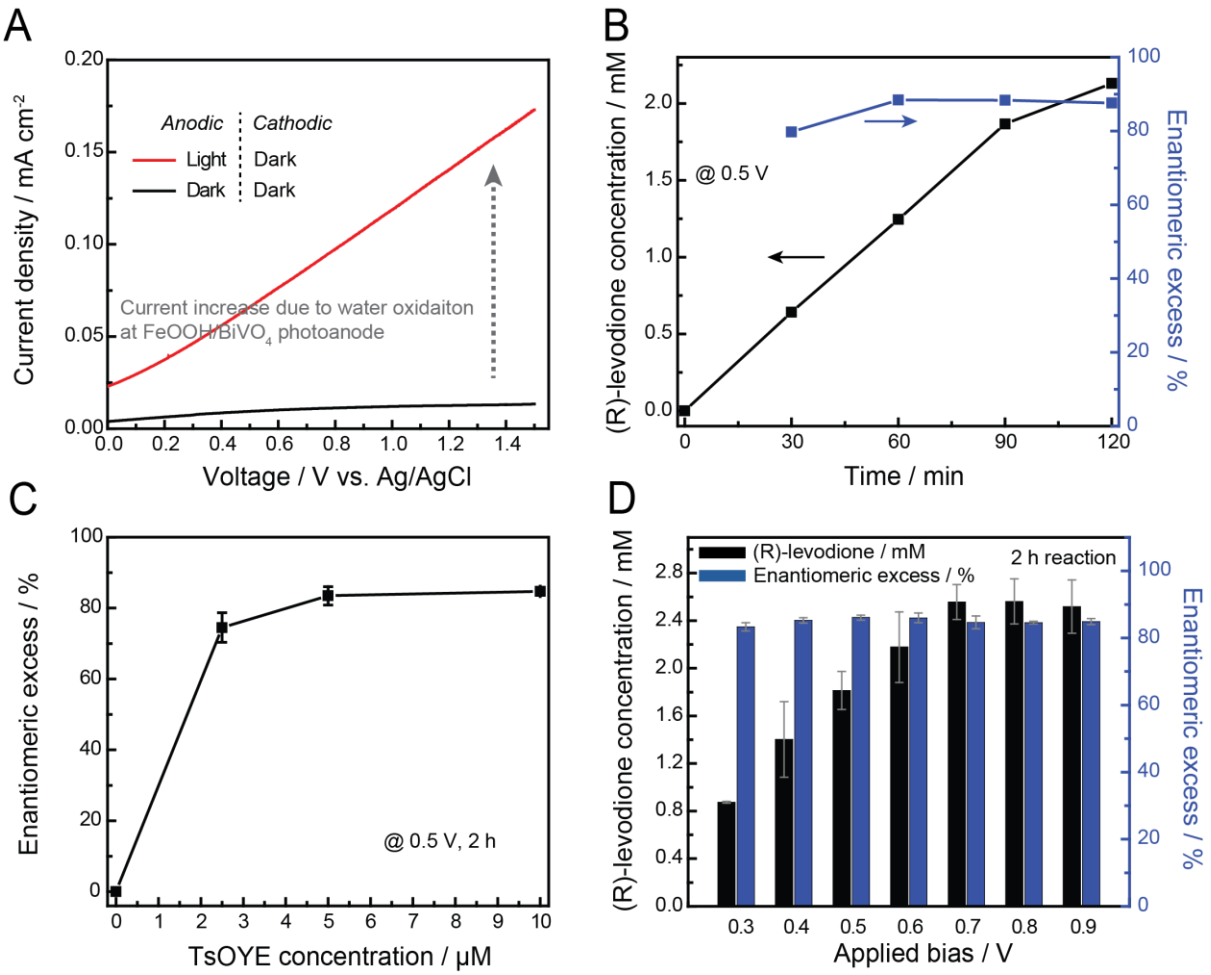

Figure 5. (A) Comparison of linear-sweep voltammograms of the full PEC composed of $FeOOH/BiVO_4$ photoanode and $CNT/p\text{-}g\text{-}C_3N_4$ cathode, with or without light illumination (> 420 nm) to the $FeOOH/BiVO_4$ side. The scan rate was 20 mV s^{-1}. (B) Time profiles of biocatalytic conversion of ketoisophorone to (R)-levodione by the full PEC under light illumination (> 420 nm) and the applied bias of 0.5 V. (C) Comparison of ee values in terms of TsOYE concentration. The test was performed for 2 h. (D) Comparison of (R)-levodione conversion yield and ee values according to different applied biases for 2 h.

Table of Contents Entry

A bio-inspired photoelectrochemical cell (PEC) configured with protonated graphitic carbon nitride (p-g-C_3N_4) and carbon nanotube hybrid (CNT/p-g-C_3N_4) film cathode and FeOOH-deposited bismuth vanadate (FeOOH/$BiVO_4$) photoanode is constructed for solar production of industrially useful chiral alkanes using an old yellow enzyme homologue from *Thermus scotoductus* (TsOYE). In the biocatalytic PEC platform, photoexcited electrons provided by the FeOOH/$BiVO_4$ photoanode are transferred to the robust and self-standing CNT/p-g-C_3N_4 hybrid film that electrocatalytically reduces flavin mononucleotide (FMN) mediator.